HCOOH Dehydrogenation on Au

DOI: 10.1002/anie.200805723

Formic Acid Dehydrogenation on Au-Based Catalysts at Near-Ambient Temperatures**

*Manuel Ojeda and Enrique Iglesia**

Formic acid (HCOOH) is a convenient hydrogen carrier in fuel cells designed for portable use.[1–4] Recent studies show that Ru-based complexes decompose aqueous HCOOH solutions at near-ambient temperatures.[5,6] Pt is the most active solid catalyst for HCOOH decomposition, at least as large crystallites and extended surfaces.[7] The identity and oxidation state of surface atoms influence the selectivity to dehydrogenation ($HCOOH \rightarrow H_2 + CO_2$) and dehydration ($HCOOH \rightarrow H_2O + CO$) routes and the ability to form CO-free H_2 streams suitable for low-temperature fuel cells. Noble metals catalyze dehydrogenation selectively, while base metals and oxides catalyze both routes, either directly or via subsequent water-gas shift (WGS).[8–11]

Formates act as intermediates in HCOOH decomposition; their formation limits rates on the nobler metals (Au, Ag) and their decomposition on the others.[10] Au catalysts give lower areal rates than other metals because of its inertness in HCOOH dissociation, evident from its first-order HCOOH decomposition kinetics.[12] Small Au clusters (<5 nm) on oxide supports catalyze many reactions, including HCOOH oxidation, at higher turnover rates than larger Au clusters, apparently because coordinatively unsaturated species of Au metal, anions, or cations bind molecules more strongly than low-index Au metal surfaces.[13–17]

Here, we show that well-dispersed Au species decompose HCOOH with metal-time yields (rates per Au atom)[18] even larger than on Pt clusters. HCOOH decomposes at near ambient temperatures ($\approx$350 K) to form only H_2 and CO_2 (<10 ppm CO), suitable for use in fuel cells. This unprecedented reactivity arises from dispersed Au species, undetected in micrographs, which grow upon thermal treatment, and not from visible metal clusters (3–4 nm), which catalyze CO oxidation and remain stable during thermal treatment.

HCOOH decomposition metal-time yields on Au/Al_2O_3 are much higher than on Pt/Al_2O_3 at 343–383 K (Figure 1).

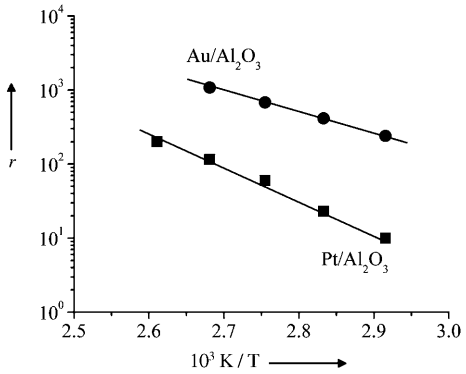

Figure 1. Arrhenius plot for HCOOH decomposition (mol h^{-1} g-at Au^{-1}) on Au/Al_2O_3 (2 kPa HCOOH) and Pt/Al_2O_3 (4 kPa HCOOH).

These differences do not reflect a distinct metal dispersion (0.28 for Au and 0.21 for Pt, estimated from clusters visible in transmission electron micrographs, TEM). Activation energies in the zero-order kinetic regime were 53 ± 2 kJ mol^{-1} and 72 ± 4 kJ mol^{-1} on Au and Pt, respectively, consistent with previous data (40–60 and 58–73 kJ mol^{-1} for Au and Pt[12,19–21]).

HCOOH dehydrogenation turnover rates increased as Pt cluster size decreased (Figure 2). Treating Au/Al_2O_3 in 20% O_2/He flow up to 1073 K strongly decreased turnover rates

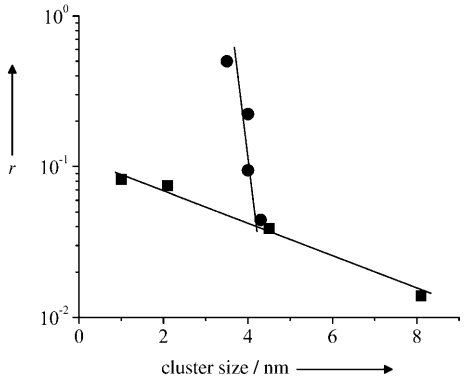

Figure 2. Turnover rates (mol s^{-1} g-at $metal_s^{-1}$) calculated from TEM-visible clusters for HCOOH decomposition on Au/Al_2O_3 (●, 2 kPa HCOOH) and Pt/Al_2O_3 (■, 4 kPa HCOOH) at 353 K.

(based on TEM-visible clusters) without concomitant changes in the size of Au clusters detected by TEM (Supporting Information). This indicates that active sites do not reside at the surfaces of these TEM-visible clusters. HCOOH dehydrogenation and WGS reactions are thought to involve

[*] Dr. M. Ojeda, Prof. E. Iglesia
Department of Chemical Engineering
University of California at Berkeley, Berkeley, CA 94720 (USA)
Fax: (+1) 510-642-4778
E-mail: iglesia@berkeley.edu
Homepage: http://iglesia.cchem.berkeley.edu

[**] M.O. acknowledges support from the European Union. The Director, Office of Basic Energy Sciences, Chemical Sciences Division of the U.S. Department of Energy also provided partial support (DE-AC02-05CH11231). H. Kung and M. Kung (Northwestern University) kindly provided the initial catalysts and the procedure required to prepare them. We thank M. Avalos Borja, L. Rendon, and F. Ruiz (UNAM, Mexico) for the TEM data shown here.

Supporting information for this article is available on the WWW under http://dx.doi.org/10.1002/anie.200805723.

common formate-type intermediates.[22,23] Not unexpectedly, WGS rates also decreased upon thermal treatment, but CO oxidation rates remain essentially unchanged (Figure 3). We

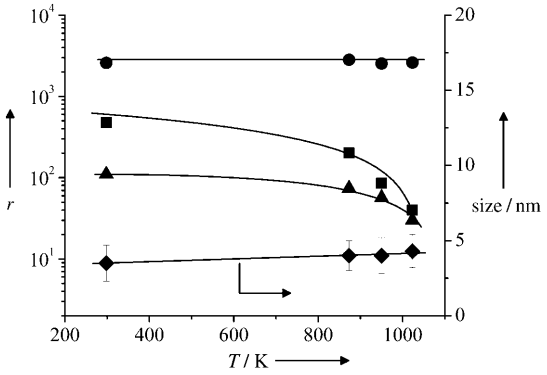

Figure 3. Influence of treatment temperature T on rates (mol h^{-1} g-at Au^{-1}) for CO oxidation (●, 288 K, 5 kPa CO, 2 kPa O_2, 0.5 kPa H_2O), HCOOH (■, 353 K, 2 kPa), water-gas shift (▲, 523 K, 5 kPa CO, 2 kPa H_2O) on Au/Al_2O_3 and Au cluster size from TEM (◆).

conclude that CO oxidation (but not WGS or HCOOH dehydrogenation) occurs on surfaces of Au clusters visible in these micrographs. HCOOH dehydrogenation and WGS require similar active sites present on much smaller Au domains (e.g. isolated Au atoms proposed in WGS on Au/CeO_2[24]). Such structures account for the very high HCOOH dehydrogenation reactivity of these Au catalysts; upon thermal treatment, they sinter to larger clusters with exposed surfaces that are much less active for HCOOH dehydrogenation and WGS.

Au/TiO_2 (treated at 523 K) shows a cluster size distribution similar to that in all Au/Al_2O_3 samples, but gave much smaller HCOOH dehydrogenation rates (7 vs. 201 mol h^{-1} g-at Au^{-1}); these data suggest that fewer isolated Au species are present on Au/TiO_2 than on Au/Al_2O_3, even after the latter was treated at 873 K. In contrast, CO oxidation rates were similar on Au/TiO_2 and all Au/Al_2O_3 catalysts (2.0–2.6 mol s^{-1} g-at Au_s^{-1}; 288 K, 5 kPa CO, 2 kPa O_2, 0.5 kPa H_2O), consistent with active sites only at the surfaces of the Au clusters detected by TEM, which are similar in size for Au/TiO_2 and Au/Al_2O_3 (3–4 nm).

Only H_2 and CO_2 were detected during HCOOH decomposition on Au/Al_2O_3, Au/TiO_2, and Pt/Al_2O_3, indicating that HCOOH dehydration and reverse WGS did not occur. Dehydrogenation rates did not depend on HCOOH pressure (0.25–8 kPa) on Au/Al_2O_3 (Figure 4). On Pt/Al_2O_3, rates increased initially with HCOOH pressure and reached constant values above 2 kPa (Figure 4). Zero-order HCOOH decomposition rates typically indicate that reactions are limited by steps involving intermediates present at saturation coverages. In this context, pathways consistent with HCOOH decomposition rate data include: A) HCOOH dissociation and either formate decomposition or hydrogen desorption kinetically-relevant steps via; B) unimolecular formate decomposition and hydrogen recombination; C) or

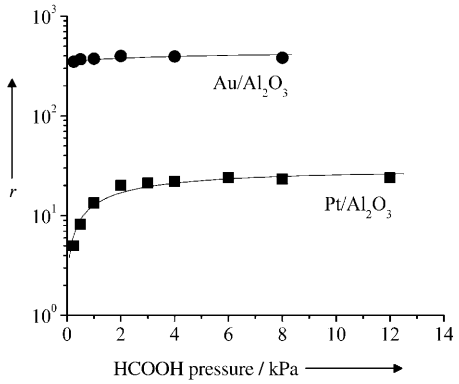

Figure 4. Effect of HCOOH partial pressure on the reaction rate (mol h^{-1} g-at $metal^{-1}$) with Au/Al_2O_3 and Pt/Al_2O_3 at 353 K.

bimolecular reactions of formate with adsorbed HCOOH molecules on distinct but saturated sites.

H/D kinetic isotope effects (KIE) were used to probe these alternate mechanistic proposals. Kinetically-relevant HCOOH dissociation would give normal KIE values ($r_H/r_D > 1$) for HCOOD, but not for DCOOH. Limiting formate decomposition would give normal KIE values for DCOOH, but not HCOOD. In contrast, limiting hydrogen desorption would give normal KIE values for both HCOOD and DCOOH. On Pt/Al_2O_3, HCOOD gave KIE values near unity, typical of thermodynamic effects, but DCOOH and DCOOD gave much larger values (Table 1); these data are

Table 1: Kinetic isotope effects for formic acid decomposition at 353 K with Pt/Al_2O_3 ($d = 0.21$, 4 kPa) and Au/Al_2O_3 ($d = 0.28$, 2 kPa).

	Pt/Al_2O_3	Au/Al_2O_3
HCOOD	1.1	1.6
DCOOH	1.7	2.5
DCOOD	2.1	4.7

consistent with kinetically-relevant via unimolecular C–H(D) bond activation steps on Pt. On Au/Al_2O_3, all isotopomers gave normal KIE values of apparent kinetic origin. These KIE values did not arise from DCOOH/HCOOD scrambling on Au or Pt catalysts. Dihydrogen isotopomers on Pt/Al_2O_3 gave binomial distributions, consistent with quasi-equilibrated recombination of H adatoms. HD was the only isotopomer detected from HCOOD or DCOOH reactions on Au/Al_2O_3, indicating that the formation of H_2 was irreversible and kinetically-relevant and that the H-atom from the OH groups desorbed only via reactions with the H-atom in the C-H group in HCOOH.

On Au/Al_2O_3, measured KIE values and dihydrogen isotopomers are consistent with the two possible mechanisms in Scheme 1. Mechanism A1 involves quasi-equilibrated O-H activation to form formates, which decompose to CO_2 and H_2 via reactions of C–H bonds in formates with H-atoms formed via O–H dissociation, before any such H-atoms recombine with others and desorb as H_2. Mechanism A2 involves formates that decompose unimolecularly, but requires that

Mechanism A1

$$1.\ HCOOH + 2^* \underset{}{\overset{K_1^{A1}}{\rightleftharpoons}} HCOO^* + H^*$$

$$2.\ HCOO^* + H^* \xrightarrow{k_2^{A1}} CO_2 + H_2 + 2^*$$

Mechanism A2

$$1.\ HCOOH + 2^* \xrightarrow{k_1^{A2}} HCOO^* + H^*$$

$$2.\ HCOO^* + {}^* \xrightarrow{k_2^{A2}} CO_2 + H^* + {}^*$$

$$3.\ H^* + H^* \xrightarrow{k_3^{A2}} H_2 + 2^*$$

Scheme 1. Plausible pathways for HCOOH dehydrogenation on well dispersed Au species.

the H-atoms formed sequentially in O–H and C–H activation recombine only with each other, without recombination with H-atoms formed in previous HCOOH decomposition turnovers. In both cases, the kinetically relevant formation of HD would lead to normal KIE values for all isotopomers and to the exclusive formation of HD from both DCOOH and HCOOD. On Pt catalysts, quasi-equilibrated recombinative hydrogen desorption scrambles hydrogen isotopomers and leads to kinetically-relevant formate decomposition steps, the rate of which depends only on the C–H/D bonds in formates.

Pathways A1 and A2 in Scheme 1 give rate equations (1) and (2) (derivation in Supporting Information):

$$r_{A1} = \frac{K_1^{A1} k_2^{A1} P_{HCOOH}[L]}{\left[1 + 2(K_1^{A1} P_{HCOOH})^{1/2}\right]^2} \quad (1)$$

$$r_{A2} = \frac{k_1^{A2} P_{HCOOH}[L]}{\left[1 + \frac{k_1^{A2}}{k_2^{A2}} P_{HCOOH} + \left(\frac{2k_1^{A2}}{k_3^{A2}}\right)^{1/2} P_{HCOOH}^{1/2}\right]^2} \quad (2)$$

respectively, when HCOO* and H* are the most abundant intermediates and [L] is the number of active sites. In the zero-order kinetic regime, they become equal to $k_2^{A1}/4$ and $k_3^{A1}/2$. The isotopic identity of both C–H and O–H groups influences k_2^{A1} and k_3^{A1}, consistent with KIE data. Mechanism A2 (but not A1) requires kinetic isolation among active sites and requires H* desorption before subsequent turnovers on a given active domain, but the A1 and A2 are otherwise indistinguishable from rate or isotopic data. We note that mechanism A2 would give identical rates for HCOOD and DCOOH dehydrogenation, because recombination occurs to form HD after cleavage of C–H/D bonds in formates. Table 1 shows KIE values of 1.6 and 2.5 for HCOOD and DCOOH, respectively. These data suggest that mechanism A1, for which rate constants reflect rates of DCOO* and H* (or HCOO* + D*) in HD formation is the more likely pathways for formic acid decomposition on dispersed Au species.

The exclusive formation of HD from HCOOD (and DCOOH) at rate proportional to k_2^{A1} (A1) or k_3^{A2} (A2) indicates that hydrogen desorption is an irreversible and kinetically-relevant step, a situation that leads to higher hydrogen chemical potentials at active sites (within any H-containing species that form H_2) than in the contacting H_2(g) as shown by non-equilibrium thermodynamic treatments of chemical kinetics.[25,26] Thus, the kinetic driving force for reactions that use hydrogen as reactants (e.g. at fuel cell electrodes or in cross-hydrogenations) would be faster during HCOOH dehydrogenation than via reactions with the H_2 pressures prevalent during HCOOH decomposition. This leads us to conclude that HCOOH can be used as an in situ hydrogen source at high chemical potentials on these isolated Au species, because active sites do not equilibrate surface and gas phase hydrogen pools during HCOOH dehydrogenation catalysis.

In summary, well-dispersed Au species undetectable by TEM dehydrogenate HCOOH with much higher metal-time yields than Pt clusters. HCOOH dehydrogenation proceeds via either a H-assisted formate decomposition mechanism or via sequential cleavage of O–H and C–H bonds and H-atom recombination on isolated sites. These reactions form H_2/CO_2 mixtures (< 10 ppm CO) suitable for fuel cells and also lead to high hydrogen chemical potentials at active sites, which are useful to hydrogenate unsaturated or O-containing molecules using HCOOH as the hydrogen source. These well-dispersed Au species also catalyze water-gas shift, but CO oxidation occurs instead on surfaces of Au metal clusters detectable by TEM.

Experimental Section

Au/Al_2O_3 (0.61 wt.%) was prepared by deposition-precipitation.[27] $HAuCl_4 \cdot x H_2O$ (0.24 g, Aldrich, 99.999%) was dissolved in deionized H_2O (80 cm^3) at 353 K. γ-Al_2O_3 (5 g, Alcoa) was treated in ambient air at 923 K for 5 h and suspended in H_2O (120 cm^3) at 353 K. Au deposition onto Al_2O_3 was performed at 353 K and a pH of 7 (adjusted with 0.5 M NaOH, Fluka, > 98%) by stirring solutions for 1 h. Solids were rinsed with deionized water (323 K) and held in ambient conditions for 24 h. Three separate aliquots were treated in O_2/He (Praxair, UHP, 25 vol.%, 25 $cm^3 g^{-1} s^{-1}$) by heating to 873 K, 950 K, or 1023 K at 0.17 $K s^{-1}$ and holding for 2 h. Au/TiO_2 (1.56 wt.%, 3.3 ± 0.7 nm) was prepared by deposition-precipitation (World Gold Council). Pt catalysts (2 wt.%) with different metal cluster size were prepared by Nanostellar using colloidal methods. HCOOH decomposition, WGS, and CO oxidation rates were measured in a packed-bed reactor using samples (30–100 mg; diluted with quartz) treated in flowing H_2 at 373 K (28 $cm^3 g^{-1} s^{-1}$, Praxair, 99.999%) for 0.5 h and in H_2O/H_2 (1 vol.% H_2O, 28 $cm^3 g^{-1} s^{-1}$) at 373 K for 0.5 h.[28] All gases (He, 10 vol.% CO/He used for WGS and CO oxidation reactions, 25 vol% O_2/He, Praxair, UHP) were metered by electronic controllers and HCOOH (Acros, 99% pure) and H_2O (deionized) were introduced with a syringe pump. Formic acid isotopomers were obtained from Cambridge Isotope Laboratories (98% isotopic purity, < 5% water). Chemical and isotopic speciation was carried out by dividing the reactor effluent into two parallel streams: one was analyzed with a mass spectrometer and the other with a gas chromatograph equipped with a Porapak Q packed column (80–100 mesh, 1.82 m × 3.18 mm) connected to a thermal conductivity detector.

Received: November 24, 2008
Revised: February 21, 2009
Published online: May 28, 2009

Keywords: formic acid · fuel cells · gold · heterogeneous catalysis · mechanism

[1] C. Rice, R. I. Ha, R. I. Masel, P. Waszczuk, A. Wieckowski, T. Barnard, *J. Power Sources* **2002**, *111*, 83 – 89.
[2] X. Yu, P. G. Pickup, *J. Power Sources* **2008**, *182*, 124 – 132.
[3] S. Enthaler, *ChemSusChem* **2008**, *1*, 801 – 804.
[4] F. Joó, *ChemSusChem* **2008**, *1*, 805 – 808.
[5] B. Loges, A. Boddien, H. Junge, M. Beller, *Angew. Chem.* **2008**, *120*, 4026 – 4029; *Angew. Chem. Int. Ed.* **2008**, *47*, 3962 – 3965.
[6] C. Fellay, P. J. Dyson, G. Laurenczy, *Angew. Chem.* **2008**, *120*, 4030 – 4032; *Angew. Chem. Int. Ed.* **2008**, *47*, 3966 – 3968.
[7] M. A. Barteau, *Catal. Lett.* **1991**, *8*, 175 – 184.
[8] J. M. Trillo, G. Munuera, J. M. Criado, *Catal. Rev.* **1972**, *7*, 51 – 86.
[9] R. Larsson, M. H. Jamroz, M. A. Borowiak, *J. Mol. Catal. A* **1998**, *129*, 141 – 151.
[10] P. Mars, J. J. F. Scholten, P. Zwietering, *Adv. Catal.* **1963**, *14*, 35 – 113.
[11] K. S. Kim, M. A. Barteau, *Langmuir* **1988**, *4*, 945 – 953.
[12] W. M. H. Sachtler, J. Fahrenfort, Actes du Deuxieme Congres Internationale de Catalyse **1961**, pp. 831–841.
[13] H. H. Kung, M. C. Kung, C. K. Costello, *J. Catal.* **2003**, *216*, 425 – 432.
[14] G. C. Bond, D. T. Thompson, *Gold Bull.* **2000**, *33*, 41 – 50.
[15] D. Andreeva, *Gold Bull.* **2002**, *35*, 82 – 88.
[16] A. S. K. Hashmi, G. J. Hutchings, *Angew. Chem.* **2006**, *118*, 8064 – 8105; *Angew. Chem. Int. Ed.* **2006**, *45*, 7896 – 7936.
[17] M. Haruta, A. Ueda, S. Tsubota, R. M. Torres Sanchez, *Catal. Today* **1996**, *29*, 443 – 447.
[18] M. Boudart, G. Djéga-Mariadassou in *Kinetics of Heterogeneous Catalytic Reactions*, Princeton University Press, Princeton, **1984**.
[19] W. J. Chun, K. Tomishige, M. Hamakado, Y. Iwasawa, K. Asakura, *J. Chem. Soc. Faraday Trans.* **1995**, *91*, 4161 – 4170.
[20] M. M. Mohamed, M. Ichikawa, *J. Colloid Interface Sci.* **2000**, *232*, 381 – 388.
[21] J. Block, J. Vogl, *Z. Elektrochem.* **1959**, *63*, 3 – 12.
[22] E. Iglesia, M. Boudart, *J. Catal.* **1983**, *81*, 214 – 223.
[23] T. Shido, Y. Iwasawa, *J. Catal.* **1992**, *141*, 71 – 81.
[24] Q. Fu, H. Saltsburg, M. Flytzani-Stephanopoulos, *Science* **2003**, *301*, 935 – 938.
[25] M. Boudart, *Catal. Lett.* **1989**, *3*, 111 – 116.
[26] S. Y. Yu, J. A. Biscardi, E. Iglesia, *J. Phys. Chem. B* **2002**, *106*, 9642 – 9648.
[27] M. Haruta, *Catal. Today* **1997**, *36*, 153 – 166.
[28] C. K. Costello, J. Guzman, J. H. Yang, Y. M. Wang, M. C. Kung, B. C. Gates, H. H. Kung, *J. Phys. Chem. B* **2004**, *108*, 12529 – 12536.

